ACS APPLIED MATERIALS & INTERFACES

Research Article

www.acsami.org

Enhanced Interfacial Interaction and CO_2 Separation Performance of Mixed Matrix Membrane by Incorporating Polyethylenimine-Decorated Metal–Organic Frameworks

Qingping Xin,[†,‡] Jingyi Ouyang,[†] Tianyu Liu,[†] Zhao Li,[†] Zhen Li,[†,‡] Yuchen Liu,[†] Shaofei Wang,[†,‡] Hong Wu,*[,†,‡,§] Zhongyi Jiang,[†,‡] and Xingzhong Cao[⊥]

[†]Key Laboratory for Green Chemical Technology, School of Chemical Engineering and Technology, and [§]Tianjin Key Laboratory of Membrane Science and Desalination TechnologyTianjin University, Tianjin 300072, China

[‡]Collaborative Innovation Center of Chemical Science and Engineering (Tianjin), Tianjin 300072, China

[⊥]Key Laboratory of Nuclear Radiation and Nuclear Energy Technology, Institute of High Energy Physics, Chinese Academy of Sciences, Beijing 100049, China

Supporting Information

ABSTRACT: Polyethylenimine (PEI) was immobilized by MIL-101(Cr) (~550 nm) via a facile vacuum-assisted method, and the obtained PEI@MIL-101(Cr) was then incorporated into sulfonated poly(ether ether ketone) (SPEEK) to fabricate mixed matrix membranes (MMMs). High loading and uniform dispersion of PEI in MIL-101(Cr) were achieved as demonstrated by ICP, FT-IR, XPS, and EDS-mapping. The PEI both in the pore channels and on the surface of MIL-101(Cr) improved the filler–polymer interface compatibility due to the electrostatic interaction and hydrogen bond between sulfonic acid group and PEI, and simultaneously rendered abundant amine carriers to facilitate the transport of CO_2 through reversible reaction. MMMs were evaluated in terms of gas separation performance, thermal stability, and mechanical property. The as-prepared SPEEK/PEI@MIL-101(Cr) MMMs showed increased gas permeability and selectivity, and the highest ideal selectivities for CO_2/CH_4 and CO_2/N_2 were 71.8 and 80.0 (at a CO_2 permeability of 2490 Barrer), respectively. Compared with the membranes doped with unfilled MIL-101(Cr), the ideal selectivities of CO_2/CH_4 and CO_2/N_2 for PEI@MIL-101(Cr)-doped membranes were increased by 128.1 and 102.4 %, respectively, at 40 wt % filler loading, surpassing the 2008 Robeson upper bound line. Moreover, the mechanical property and thermal stability of SPEEK/PEI@MIL-101(Cr) were enhanced.

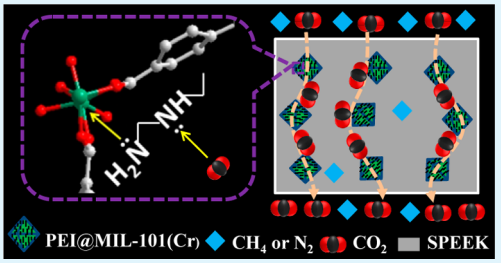

KEYWORDS: *sulfonated poly(ether ether ketone), MIL-101(Cr), polyethylenimine, uniform dispersion, facilitated CO_2 transport, mixed matrix membranes*

1. INTRODUCTION

Membrane processes have received increased attention because of their advantages such as lower energy costs, small footprint and environmental sustainability over other conventional methods for gas separation.[1] Pure polymer gas separation membranes suffer from a trade-off effect between permeability and selectivity, i.e., polymers with high selectivity present low permeability and vice versa.[2,3] The combination of polymeric membrane materials and inorganic particles to fabricate the so-called mixed matrix membranes (MMMs) have been widely investigated for gas separation aiming to surpass to the intrinsic trade-off limit.[4−7] For instance, adding inorganic fillers into polymer membranes often leads to improvements in gas permeability without scarifying selectivity or even in some cases simultaneously improving gas selectivity compared to the corresponding unfilled polymer membranes.[8,9]

During the past decades, mixed matrix membranes (MMMs) for gas separation have been investigated with different kind of inorganic fillers.[10−15] Zeolites,[10,11] activated carbons,[12] silicas,[13] and new classes of porous materials[14,15] have been investigated for their favorable CO_2 adsorption ability. Among them, metal–organic frameworks (MOFs) with high porosity, strong affinity toward certain gas molecules, and good thermal stability are emerging as one of the most promising gas adsorbent candidates. The adsorption selectivity and CO_2 uptake of MOFs is found to be much higher than those of zeolites.[16] Currently, there are hundreds of crystalline MOFs available, which have shown promising potential applications in gas adsorption and separation. However, MOFs have not been well studied as fillers to produce MMMs for gas separation yet. There are only a few research reports about MMMs containing MOFs or COFs (covalent organic frameworks).[17−27] Most related research has revealed a high degree of MOF/polymer adhesion because organic linkers in MOFs have a good affinity

Received: July 19, 2014
Accepted: December 19, 2014
Published: December 19, 2014

DOI: 10.1021/am504742q
ACS Appl. Mater. Interfaces 2015, 7, 1065−1077

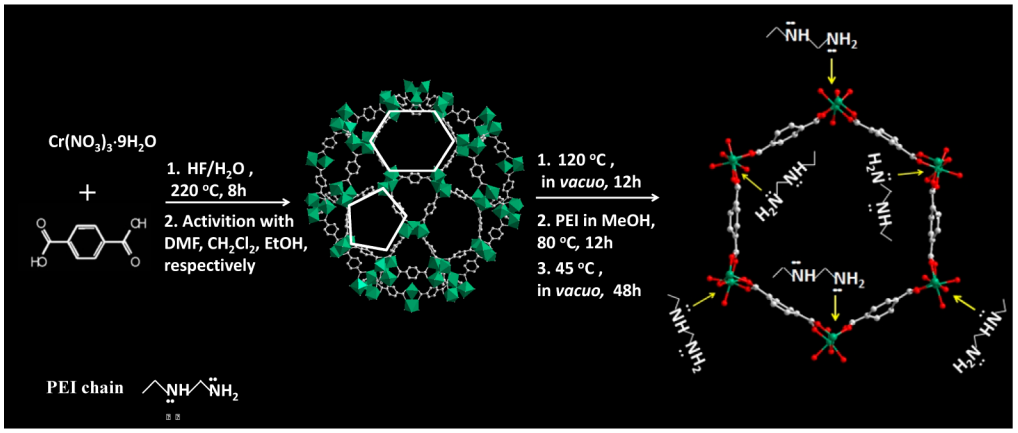

Figure 1. Scheme for the synthesis of the PEI-decorated MIL-101(Cr) (PEI@MIL-101(Cr)). The framework structure depicted is obtained from single crystal X-ray analysis of the MIL-101(Cr). Green, red, and gray spheres represent Cr, O, and C atoms, respectively; H atoms are omitted for clarity.

with polymer chains, and the surface properties of MOFs can be tuned by functionalization with various organic molecules if necessary.[24] Although MOF fillers can overcome the problem of phase separation and the surface void between two phases, the gas separation properties of MOF/polymer type MMMs would not be the simple combination of both advantages. Further successful development of MMMs depends on several factors, such as the proper selection of MOF/polymer pair and the elimination of interfacial defects between the two phases. As a new kind of MOF, the so-called MIL (Materials of Institut Lavoisier) series show high thermal and chemical stability.[28,29] Because of their organic linkage, these porous materials are of potential use in MMMs with particular interest in applications for such as CO_2 capture.[30,31] The MIL-101(Cr) is not only highly stable, but also has very large mesoporous cages of 29 and 34 Å and exhibits high CO_2 uptake of 40 mol kg^{-1} (304 K, 5 MPa). Recently, Jeazet et al.[32] incorporated MIL-101 (Cr) into polysulfone (PSF) and results showed an unsurpassed O_2 permeability increase by a factor of 6 times at fillers loading of 24 wt %. The incorporation of functionalized MOFs (NH_2-MIL-53(Al)) as fillers into different polymers such as polysulfone and polyimide showed excellent interfacial compatibility, allowing loadings up to 32 wt %.[27,33]

MOFs decorated with amine groups were investigated for efficient gas transport and separation.[34−38] Nair et al. found that the amine groups incorporated into zeolitic imidazolate frameworks (ZIFs) could improve the adsorption selectivity for CO_2/CH_4.[34] Couck et al. demonstrated that the MIL-53(Al) metal−organic framework functionalized with amino groups increased CO_2/CH_4 selectivity by orders of magnitude.[35] Janiak et al. reported that amine-modified MIL-101(Cr) showed an enhanced CO_2 adsorption as well as high CO_2/N_2 and CO_2/CH_4 selectivity of 119 and 75, respectively. Compared with unmodified MIL-101(Cr), the favorable CO_2 adsorption on amine-modified MIL-101(Cr) was due to the presence of the Lewis basic amine groups.[36] Hu et al. functionalized MIL-101(Cr) with alkylamine molecules and acquired a significantly improved CO_2 adsorption capacity as well as ultrahigh CO_2/N_2 selectivity due to the interaction between amine groups and CO_2 molecules.[37] Yan et al. prepared dual amine-decorated metal−organic framework adsorbents with tunable porosity and found that the adsorbents exhibited remarkable CO_2/CH_4 selectivity and CO_2 adsorption capacity at low pressures.[38]

Recently, SPEEK (sulfonated poly(ether ether ketone)) has been used to gas separation and was shown to be a promising polymer material.[39,40] Amine- functionalization is deemed as a viable solution to further enhance the CO_2 capture ability of MOFs. However, previous studies showed that direct chemical modification of aromatic amine groups onto MOFs only resulted in slightly enhanced CO_2 adsorption and CO_2/CH_4 selectivity.[38] In this study, MIL-101(Cr) with a particles size of ∼550 nm and good water/moisture stability was chemically decorated with polyethylenimine (PEI) rich in amine groups. Here, PEI with a relatively low molecular weight (300 Da) was chosen because it could readily penetrate into the mesoporous cages of MIL-101(Cr). In order to facilitate the diffusion of polyamines into their pores, a facile vacuum-assisted method was used to decorate PEI onto MIL-101(Cr). The as-prepared PEI-decorated MOFs were incorporated into SPEEK to fabricate MMMs for gas separation. First, the inherent high permeability of MOFs with high porosity was expected to optimize fractional free volume and enhance the gas permeability of MMMs. Second, the organic molecules were loaded into fillers to improve the filler−polymer interface compatibility. Third, the introduction of MOFs decorated with abundant amine groups into membrane was expected to facilitate the transport of CO_2 through reversible reaction between CO_2 and amine groups and lead to increased CO_2/gas reaction selectivity. The membrane morphology, polymer chain rigidity, free volume property, mechanical property and thermal stability were characterized and the gas separation performance was investigated for CO_2/CH_4 and CO_2/N_2 mixtures.

2. MATERIALS AND METHODS

2.1. Synthesis of MIL-101(Cr) and Impregnation of PEI into MIL-101(Cr). MIL-101(Cr) was prepared by a hydrothermal reaction following the procedure as reported by Férey and co-workers.[28,29] The open windows and the mesoporous cages of MIL-101(Cr) in the 3D framework are shown in Figure S2 in the Supporting Information. The detailed synthesis was as follows: chromic nitrate (800 mg, 2 mmmol), terephthalic acid (332 mg, 2 mmol), hydrofluoric acid (0.413 mL) and deionized water (10 mL) were mixed in a Teflon-lined stainless steel autoclave and kept at 220 °C for 8 h. After the synthesis, the autoclave reactor was slowly cooled down to room temperature for 3 h. The solution was then filtered and the nanocrystals were washed with DMF, EtOH and CH_2Cl_2 solvents for activation or evacuation of guest molecules from the pores of the material. The obtained crystal was designated as MIL-101(Cr).

DOI: 10.1021/am504742q
ACS Appl. Mater. Interfaces 2015, 7, 1065−1077

PEI was impregnated into MIL-101(Cr) via a facile vacuum-assisted method (VAM) by the following steps.[38] Taking large cage and hexagonal windows for example, the synthesis of the PEI-decorated MIL-101(Cr) is shown in Figure 1. First, MIL-101(Cr) was placed in a Schlenk tube under vacuum at 120 °C for 12 h. Second, PEI solution (20 mL) and anhydrous methanol (20 mL) were added into the Schlenk tube under vacuum at 80 °C and afterward vacuum was removed and the mixture was stirred for 12 h. Third, the PEI impregnated MIL-101(Cr) was centrifuged, washed by water until the pH of supernatant liquid was neutral, and dried at 45 °C under vacuum until constant weight. Finally, a brown powder was obtained, which was designated as PEI@MIL-101(Cr).

2.2. Preparation of Membranes. The membranes were fabricated by the solution-casting method. The as-prepared SPEEK (0.6 g) was dissolved in DMAc (12 mL) and a desired amount of MIL-101(Cr) or PEI@MIL-101(Cr) was dispersed into the solution homogeneously. The mixture was cast onto a glass plate, kept at 60 °C for 12 h, and then kept at 80 °C for another 12 h. The MMMs were named after SPEEK/MIL-101(Cr)-X or SPEEK/PEI@MIL-101(Cr)-X, where MIL-101(Cr) or PEI@MIL-101(Cr) referred to the MOF filler in MMMs, respectively, and X referred to the weight percentage of MIL-101(Cr) or PEI@MIL-101(Cr) relative to SPEEK. Unfilled SPEEK membrane was prepared for comparison. The thickness of the as-prepared flat sheet homogeneous membranes was in the range of 50−80 μm to ensure sufficient mechanical strength for gas separation test.

2.3. Characterization. *2.3.1. Characterization of MIL-101(Cr) and PEI@MIL-101(Cr).* The leakage ratio of PEI was tested in periodic-replacement water at 80 °C. PEI@MIL-101(Cr) was immersed in 10 mL deionized water at 80 °C for 5 days, and then PEI@MIL-101(Cr) was centrifuged from supernatant liquid. The obtained PEI@MIL-101(Cr) was immersed in 10 mL fresh deionized water at 80 °C for another 5 days and the supernatant liquid was tested by ICP to detect the content of nitrogen element. The aforementioned procedures were in loop execution. The leakage ratio of PEI was calculated by the following equations.

$$m_n = V\frac{\omega_n M_{PEI}}{n_N M_N} \quad (1)$$

$$L_n = \frac{(\sum_{j=1}^{n} m_j)}{m_{PEI}\omega_{PEI}} \quad (2)$$

where ω_n (wt %, g mL^{-1}) was the content of nitrogen element of supernatant liquid separated after the nth circle, V was the volume of water (mL), M_{PEI} (g mol^{-1}) and M_N (g mol^{-1}) were relative molecular mass of PEI and relative atomic mass of nitrogen, respectively, n_N was the number of nitrogen in PEI (n_N =7), m_n (g) was the leakage of PEI in the nth circle, Σ was a summation notation and was employed to calculate the total leakage of PEI after the nth circle, m_{PEI} was the initial weight of PEI@MIL-101(Cr), ω_{PEI} (wt %, g g^{-1}) was the PEI content of PEI@MIL-101(Cr) determined by ICP as described in section characterizations of MIL-101(Cr), L_n (%) was leakage ratio of PEI after the nth circle.

2.3.2. Characterization of Membranes. Positron annihilation lifetime spectroscopy (PALS) of the flat sheet homogeneous membranes was recorded with an ORTEC fast−fast coincidence system (the resolution was 201 ps) to investigate the free volume property of the membranes. The positron source-22Na was sandwiched between two pieces of samples with a thickness range of 0.5−0.6 mm. The spectra with more than one million counts were recorded and then resolved by LT-v9 program. On assumption that the location of o-Ps occurs in a sphere potential well surrounded by an electron layer of a constant thickness Δr (0.1656 nm), radius of free volume cavity (r_3) was calculated from the pick-off annihilation lifetime of o-Ps (τ_3) by the following semiempirical eq 3.

$$\tau_3 = \frac{1}{2}\left[1 - \frac{r_3}{r_3 + \Delta r} + \left(\frac{1}{2\pi}\right)\sin\left(\frac{2\pi r_3}{r_3 + \Delta r}\right)\right]^{-1} \quad (3)$$

The apparent fractional free volume (FFV) of the equivalent sphere could be calculated using eq 4.

$$FFV = \frac{4}{3}\pi r_3^3 I_3 \quad (4)$$

2.4. Gas Separation Performance of Membranes. Pure gas (CO_2, CH_4, and N_2) and mixed gas (CO_2/CH_4 (30 vol %: 70 vol %), CO_2/N_2 (10 vol %: 90 vol %)) permeation measurements were conducted at 25 °C based on the conventional constant pressure/variable volume technique. The gas transport properties of the flat sheet homogeneous membrane were measured using a flat sheet permeation cell which was placed in a thermostat oven to control the experimental temperature (see Figure S3 in the Supporting Information). N_2 was used as the sweep gases for CO_2/CH_4 mixed gas and CH_4 pure gas as feed gases, whereas CH_4 was applied for CO_2/N_2 mixed gas, CO_2 pure gas and N_2 pure gas as feed gases, respectively. In a typical measurement, both feed gas and sweep gas were introduced into a water bottle (35 °C) to be saturated with water vapor. For comparison, dry-state gas permeation experiments were also conducted, in which case the feed gas and sweep gas were directly introduced into the membrane cell. The flow rates of the feed gas and the sweep gas used for testing the membrane performance were controlled by mass flowmeters and fixed at 200 cm^3 (STP)/min and 45 cm^3 (STP)/min, respectively. The sweep side (the permeate gas together with the sweep gas) was sent to a gas chromatograph (Agilent 6820 gas chromatography equipped with a thermal conductive detector (TCD)) to determine the proportion of each component. Therefore, using the flow rate of sweep gas (F_{sweep}) and its composition (x_{sweep}), the total flow rate (F_{total}) of the sweep side gas could be calculated by $F_{total} = F_{sweep}/x_{sweep}$, the flow rate of the permeate gas ($F_{permeate}$) could be calculated by $F_{permeate} = F_{total}x_{permeate}$.The permeability ($P_i$, Barrer, 1 Barrer equals 1×10^{-10} cm^3 (STP) cm/(cm^{2}s cmHg)) of each gas was measured and each set of data was obtained from at least three tests. P_i was determined by the equation: $P_i = Q_i l/\Delta p_i A$, where Q_i was the volumetric flow rate of gas 'i' (cm^3/s (SPT)), l was the thickness of the membranes measured by a micrometer calliper (μm). Δp_i was the transmembrane pressure difference (cmHg), and A was the effective membrane area, 12.5 cm^2. The ideal selectivity and mixed gas separation factor of gas "i and j" ($\alpha_{i/j}$) was calculated by $\alpha_{i/j} = P_i/P_j$. To further elucidate the change in membrane separation performances, we measured diffusivity and solubility coefficients of flat sheet homogeneous membranes by the time-lag method[39] at 25 °C and the upstream side was maintained at 1.5 bar. Before analysis, the membranes were evacuated at least 8 h to remove previously dissolved species. For each membrane, the gases were tested in the order of N_2, CH_4, and CO_2.

3. RESULTS AND DISCUSSION

3.1. Characterization of MIL-101(Cr) and PEI@MIL-101(Cr). As shown in Figure S4 in the Supporting Information, scanning electron microscopy (SEM) images indicated that the morphologies and sizes of MIL-101(Cr) after PEI decoration remained nearly intact. Approximate octahedral crystals with a uniform size of about 550 nm could be observed. The PEI@MIL-101(Cr) structure was slightly changed after PEI was loaded into the pores.

Powder X-ray diffraction (PXRD) patterns (see Figure S5 in the Supporting Information) showed that the Bragg diffraction angles in MIL-101(Cr) and PEI-decorated MIL-101(Cr) were essentially identical, confirming the relatively intact MIL-101(Cr) crystalline structure after loading PEI. However, it could be seen that the intensity of the peaks below 6° was reduced. This was attributed to the filling of MIL-101(Cr) pores by PEI, which decorated the pore properties, such as pore size and polarity.

The successful impregnation of PEI was verified by FT-IR, EDX, and XPS as shown in Figure S6a−c in the Supporting

DOI: 10.1021/am504742q
ACS Appl. Mater. Interfaces 2015, 7, 1065−1077

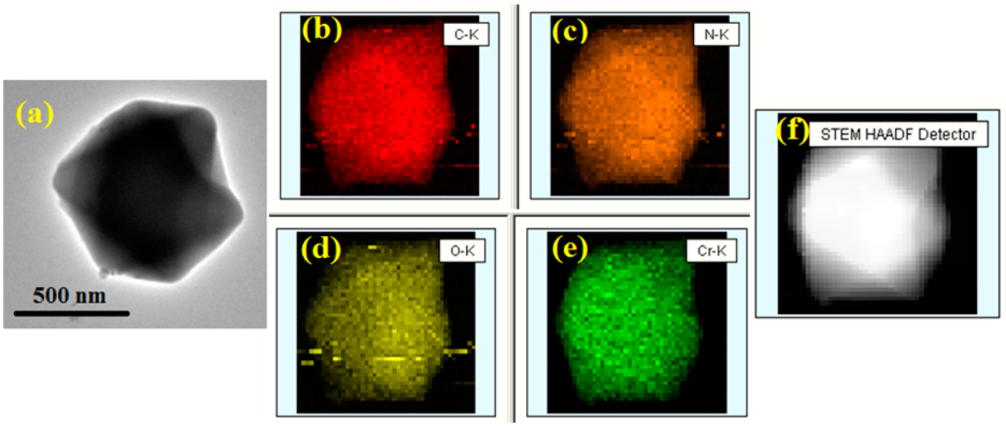

Figure 2. Elemental distribution of PEI@MIL-101(Cr) probed by EDS-mapping: (a) FETEM imagine of PEI@MIL-101(Cr); (b) distribution of carbon, (c) distribution of nitrogen; (d) distribution of oxygen; (e) distribution of chromium; (f) STEM image displaying high-angle angular dark-field (HAADF) detector.

Information, respectively. FT-IR spectrum of PEI-decorated MIL-101(Cr) sample clearly showed the representative peaks between 3500 and 2800 cm^{-1} corresponding to n(NH) and n(CH) stretching vibrations of PEI (see Figure S6a in the Supporting Information).

The distribution of PEI in MIL-101(Cr) was observed by the EDS-mapping and inferred by the comparison between the result of ICP and XPS. The EDS-mapping shown in Figure 2 reveals the distribution of N in PEI@MIL-101(Cr), with the distribution of carbon (C), chromium (Cr), and oxygen (O) as comparison. It could be clearly observed that N was of uniform distribution, which was further confirmed by the similar N content in the entire MIL-101(Cr) (19.69 wt %, detected by ICP; 17.49 at %, detected by EDS shown in Figure S6b in the Supporting Information) and on the surface of MIL-101(Cr) (18.35 at %, detected by XPS shown in Figure S6c in the Supporting Information).

The contents of nitrogen in PEI@MIL-101(Cr) was directly measured by elementary analysis (EA) to be 6.9 wt %. The thermal stability of MIL-101(Cr) and PEI@MIL-101(Cr) was characterized by TGA and shown in Figure S6d in the Supporting Information. Two weight-loss steps were observed. The initial weight loss step before 135 °C was due to the loss of adsorbed water. The second weight loss stage between 230 and 700 °C was attributed to the decomposition of the functional groups and the framework of MOF, 50 and 72 wt % for MIL-101(Cr) and PEI@MIL-101(Cr) respectively. The content of PEI in PEI@MIL-101(Cr) was indirectly calculated to be 22 wt %, and 22 wt % PEI resulted in 7 wt % nitrogen, which was identical to the elemental analysis result. Both MIL-101(Cr) and PEI@MIL-101(Cr) were thermally stable up to 235 °C.

The surface area, pore volume, and pore size of the particles after PEI modification were measured by N_2 adsorption isotherm at 77.3 K (see Figure S7 in the Supporting Information). After PEI modification, the surface area, pore volume, and pore size decreased from 3175 $m^2\ g^{-1}$, 2.28 $cm^3\ g^{-1}$, and 0.753 nm for MIL-101(Cr) to 1372 $m^2\ g^{-1}$, 0.929 $cm^3\ g^{-1}$, and 0.661 nm for PEI@MIL-101(Cr). The significantly decreased N_2 adsorption amount and surface area as well as the modestly reduced pore size verified that PEI not only decorated inner pores of MOFs but also blocked the pores of MOFs.

3.2. Characterization of Membranes. The cross-section morphology of SPEEK/MIL-101(Cr) MMMs and SPEEK/PEI@MIL-101(Cr) MMMs at different amount of MOFs (~550 nm) loadings was characterized by SEM (Figure 3). Because of the flexible SPEEK polymer chains and the similar physicochemical properties between MOFs fillers and polymer matrix, both the MIL-101(Cr) and the PEI@MIL-101(Cr) particles were wrapped tightly by the chains of SPEEK, resulting in good compatibility between MOF fillers and SPEEK matrix. Both MIL-101(Cr) and PEI@MIL-101(Cr) dispersed well in mixed matrix membranes at the MOFs contents up to 40 wt %.

FTIR spectra of flat sheet homogeneous mixed matrix membranes are shown in Figure 4. The major vibration peaks associated with the O═S═O of unfilled SPEEK membrane at 1022, 1078, and 1225 cm^{-1} were found in all the mixed matrix membranes. Compared with unfilled SPEEK membrane, the mixed matrix membranes exhibited higher peak intensity at 1650 cm^{-1}, attributed to the vibration of heteroaromatic ring in MIL-101(Cr). Moreover, the FTIR spectrum of the membrane loaded with PEI-decorated MIL-101(Cr) clearly showed the representative peaks between 3500 and 2800 cm^{-1} corresponding to the n(NH) and n(CH) stretching vibrations in the incorporated PEI. The peaks at 3415 and 3267 cm^{-1} (related to the n(NH) in PEI) were shifted to low wave numbers 3394 and 3070 cm^{-1}, respectively, indicating that hydrogen bonding emerged between sulfonic acid groups and amine groups after the incorporation of PEI@MIL-101(Cr) due to the formation of S═O···H−N. In addition, −S−OH groups were deprotonated to generate −S−O^- group in the presence of amine groups.[41,42] The deprotonated protons would protonate the nitrogen atoms of amine group, producing the attractive interactions between amine groups and SPEEK in the form of −S−O^-···$^+$H-HN− and −S−O^-···$^+$H−N =.[43,44] In summary, sulfonic acid-amine groups pairs (acid−base pairs) formed at PEI@MIL-101(Cr)-SPEEK interface.

The glass transition temperatures (T_g) of flat sheet homogeneous membranes were determined by DSC measurement to study the mobility of polymer chains (see Figure S9 in the Supporting Information). The T_g of unfilled SPEEK membrane was 153.6 °C. The T_g values of the mixed matrix membranes increased with increasing filler loading, and the T_g values of the SPEEK/PEI@MIL-101(Cr) (from 154.3 to 165.9 °C) were higher than those of the SPEEK/MIL-101(Cr) membranes (from 155.5 to 161.2 °C) with the increased filler contents from 10 to 40 wt %. It could be concluded that the incorporation of PEI@MIL-101(Cr) to the polymer matrix

DOI: 10.1021/am504742q
ACS Appl. Mater. Interfaces 2015, 7, 1065−1077

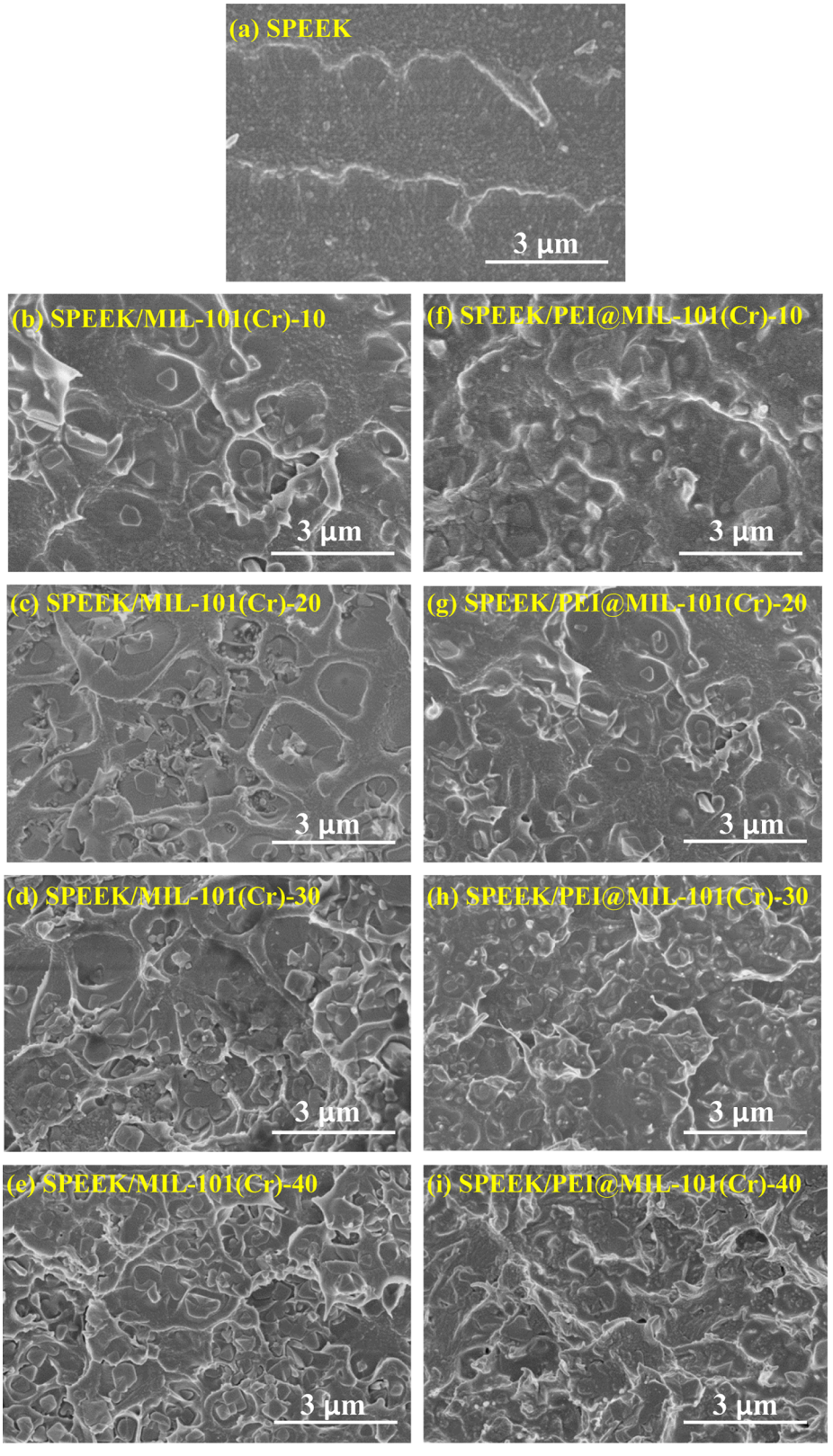

Figure 3. FESEM images of the cross-section of membranes: (a) unfilled SPEEK membrane, (b) SPEEK/MIL-101(Cr)-10, (c) SPEEK/MIL-101(Cr)-20, (d) SPEEK/MIL-101(Cr)-30, (e) SPEEK/MIL-101(Cr)-40, (f) SPEEK/PEI@MIL-101(Cr)-10, (g) SPEEK/PEI@MIL-101(Cr)-20, (h) SPEEK/PEI@MIL-101(Cr)-30, and (i) SPEEK/PEI@MIL-101(Cr)-40.

generated stronger interactions and resulted in higher polymer chain rigidification at the filler−polymer interface than that for MIL-101(Cr). The increased T_g values of SPEEK/PEI@MIL-101(Cr) membranes were attributed to the interactions (hydrogen bonds and electrostatic interaction) in the interfacial regions between SPEEK matrix and PEI@MIL-101(Cr), which constrained the motions of polymer chains, leading to further increased T_g.

DOI: 10.1021/am504742q
ACS Appl. Mater. Interfaces 2015, 7, 1065−1077

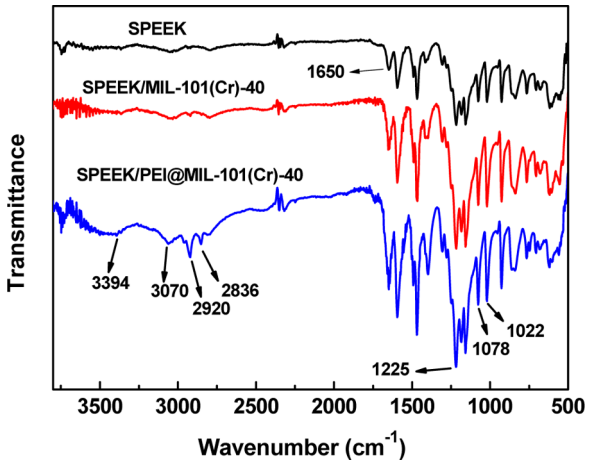

Figure 4. FTIR of membranes.

The free volume parameters of the flat sheet homogeneous membranes are characterized as listed in Table S1 in the Supporting Information. Compared with the unfilled SPEEK membrane, the fractional free volumes (FFV) of both SPEEK/MIL-101(Cr) membranes and SPEEK/PEI@MIL-101(Cr) membranes were increased and the size of the free volume cavities (r_3) of these membranes was slightly changed. Moreover, the fractional free volume (FFV) decreased for SPEEK/PEI@MIL-101(Cr) membranes compared with SPEEK/MIL-101(Cr) membranes at the same filler loading. This decreased FFV was due to the electrostatic attraction between the amino groups in PEI and the sulfonic acid groups in SPEEK.

TGA of membranes is carried out to investigate the influence of incorporation of MOFs on the thermal stability of membranes as shown in Figure S10 in the Supporting Information. All the membranes showed major three-stage weight loss. The first-stage (30−150 °C) weight loss was attributed to the evaporation of residual solvent and adsorbed water. The second-stage (230−375 °C) weight loss was ascribed to the decomposition of the $-SO_3H$ groups and the organic compound from MOFs. The third-stage (390−800 °C) weight loss was due to the degradation of the polymer main chains. It could be seen that the thermal decomposition process of membranes was modestly affected by the incorporation of MIL-101(Cr) and PEI@MIL-101(Cr), leading to an enhanced thermal stability.

Water uptake and area swelling of membranes are measured as shown in Figure S11 in the Supporting Information. Compared with the unfilled SPEEK membrane, both the water uptake and the area swelling of the MMMs increased from 9.5 and 4.9 % for unfilled SPEEK to 28.3 and 13.2 % for SPEEK/PEI@MIL-101(Cr)-40 membrane, respectively. These increases were attributed to the increased free volume and r_3 of the MMMs after incorporation of MOFs fillers. The time-dependent mixed gas CO_2 separation properties of SPEEK and SPEEK/PEI@MIL-101(Cr) membranes in wet state were plotted in Figure S12 in the Supporting Information, and the gas separation performance of membranes was slightly changed in 1.5 h.

3.3. Pure Gas Separation Performance. To meet the requirement on permeability in practical application, the membrane thickness can be reduced by fabricating asymmetric composite membrane in which the membrane material is cast on some specific support membrane to ensure mechanical strength. Pure gas permeation tests were performed to probe the intrinsic gas transport properties of membrane materials. As shown in Figure 5, all flat sheet homogeneous mixed matrix membranes exhibited performance superior to the unfilled SPEEK membrane under humidified state, and the humidified membranes doped with PEI@MIL-101(Cr) outperformed those doped with MIL-101(Cr). Especially, the membranes doped with PEI@MIL-101(Cr) displayed the highest selectivities of 71.8 and 80.0 for CO_2/CH_4 and CO_2/N_2, respectively, with a CO_2 permeability of 2490 Barrer, which were significantly higher than those of unfilled SPEEK. Most of the performance data of humidified membranes surpassed the upper bound reported in 2008, whereas those of the dry membrane fell far below that line. From another viewpoint, both permeability and selectivity were significantly enhanced after humidication for MMMs, while humidication did not obviously improve the selectivity of unfilled SPEEK. It was inferred that water content, open metal sites and amine groups contributed to the above encouraging results as discussed below. The effect of filler content on the membrane structure and performance were also elucidated in the following section.

The total water, free water and bound water of all flat sheet homogeneous membranes were analyzed to pursue rational explanation of the separation performance of MMMs. As shown in Figure 6a, the membranes doped with PEI@MIL-101(Cr) contained higher amounts of water (especially bound water) than other membranes. Panels b and c in Figure 6 clearly reveal the relationship between the water uptake and

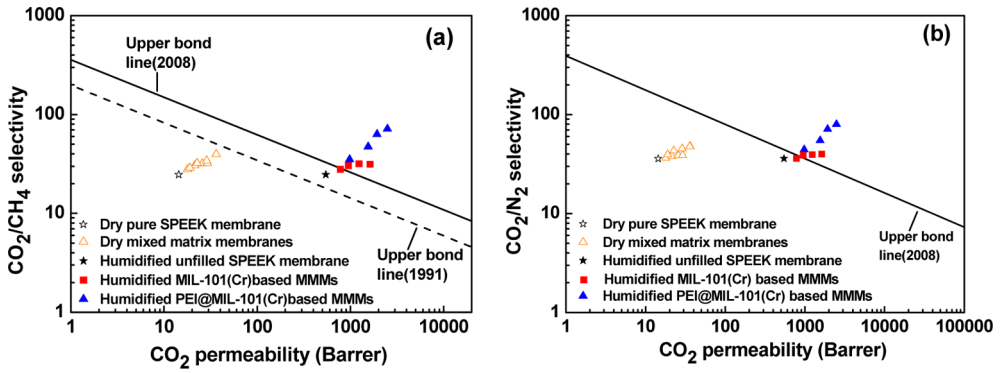

Figure 5. Pure gas separation performance of the membranes for (a) CO_2/CH_4 and (b) CO_2/N_2 mixtures, respectively (temperature, 25 °C; pressure, 1 bar).

DOI: 10.1021/am504742q
ACS Appl. Mater. Interfaces 2015, 7, 1065−1077

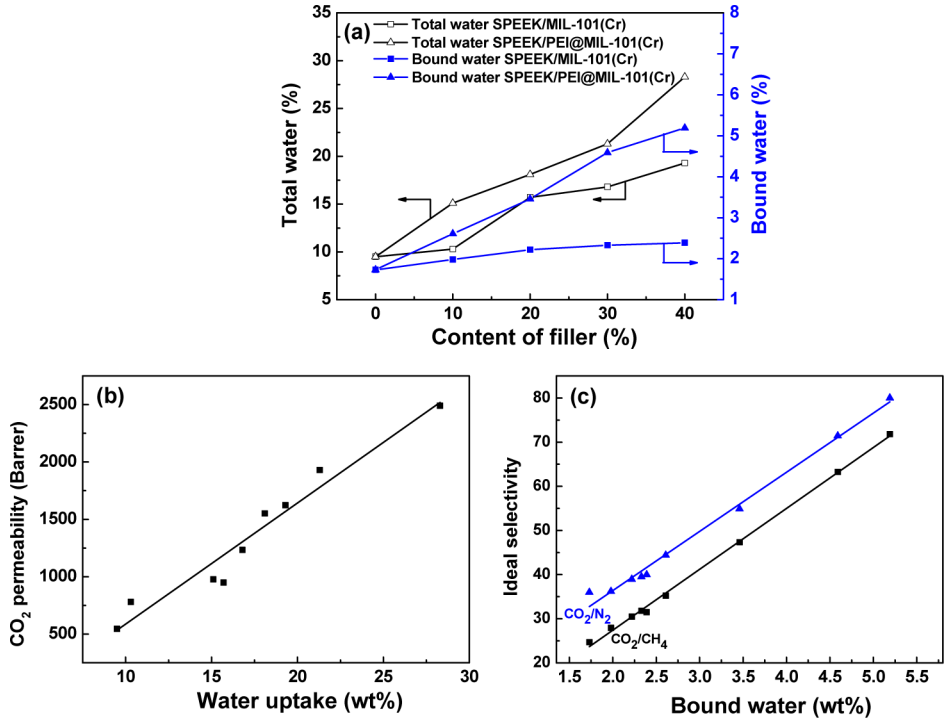

Figure 6. (a) Content of total water and bound water of the humidified membranes, (b) correlations between pure gas CO_2 permeability and water uptake in the membranes, and (c) correlations between pure gas CO_2/CH_4, CO_2/N_2 selectivity and bound water content in the membranes.

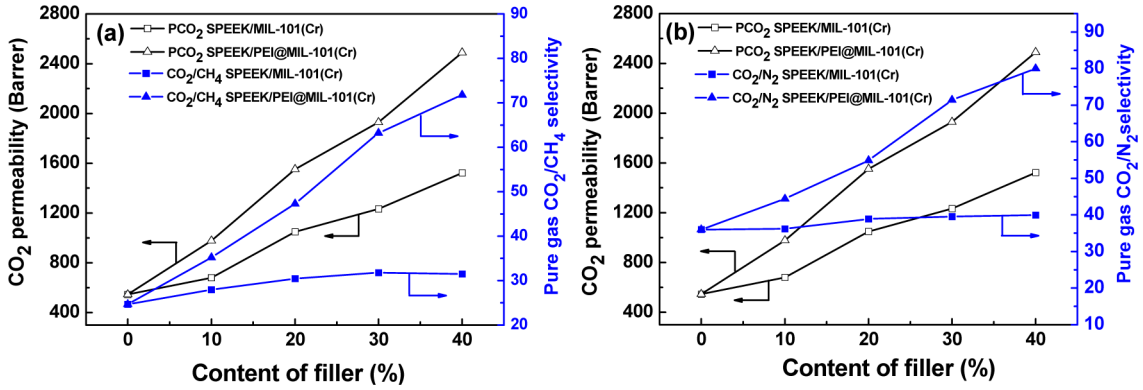

Figure 7. (a) Pure CO_2 permeability and CO_2/CH_4 selectivity; (b) pure CO_2 permeability and CO_2/N_2 selectivity for unfilled MIL-101(Cr) and PEI@MIL-101(Cr) based MMMs (1 bar, 25 °C).

CO_2 separation performance: high W_t led to high CO_2 permeability, and high W_b corresponded to high CO_2/gas selectivity. It can be easily understood that high W_t plasticized the polymer chains and led to high CO_2 permeability. In addition, the FTIR spectra of flat sheet homogeneous membranes after absorption and desorption of CO_2 are shown in Figure S13 in the Supporting Information. The dry membranes (A, D, G) and the humidified membranes after desorption of CO_2 (C, F, I) and the humidified membranes after absorption of CO_2 (B, E) showed quite similar spectra. However, the humidified SPEEK/PEI@MIL-101(Cr)-40 membrane after absorption of CO_2 (H) showed new bands. The bands at 839 and 963 cm^{-1} were assigned to the characteristic absorption bands of HCO_3^- produced by CO_2, amine groups and water, and the sharp band at 2346 cm^{-1} was attributed to the complexes of $RHNCOO^-$ or R_2NCOO^-.[45,46]

In summary, the water binding with the amide groups from PEI@MIL-101(Cr) facilitated the hydration of CO_2 and the generation of HCO_3^-, which was able to permeate through the MMMs with much lower energy barrier.

The gas separation performance of the unfilled SPEEK membrane and the MMMs was tested for CO_2/CH_4 and CO_2/N_2 mixtures (Figure 7). The CO_2 permeability increased from 545 Barrer for unfilled SPEEK to 2490 Barrer for SPEEK/PEI@MIL-101(Cr) membrane at 40 wt % loading. The ideal CO_2/CH_4 selectivity and the ideal CO_2/N_2 selectivity increased from 24.7 and 36.0 for unfilled SPEEK to 71.8 and 80.0 for SPEEK/PEI@MIL-101(Cr) membrane at 40 wt % loading, respectively. The CO_2 permeability of the MMMs was significantly higher than that of the unfilled SPEEK membrane and the increase was in proportion to the filler loading (0−40 wt %), confirming the positive effect of the filler on the membrane performance. The increase in permeability was attributed to the higher intrinsic permeability of the filler as compared to the polymer. Moreover, the enhanced CO_2 permeability of SPEEK/MIL-101(Cr) MMMs might be

DOI: 10.1021/am504742q
ACS Appl. Mater. Interfaces 2015, 7, 1065−1077

Table 1. Gas Diffusivity and Solubility Coefficients of the Membranes[a]

membrane	D_{CO2} [b]	D_{CH4} [b]	D_{N2} [b]	S_{CO2} [c]	S_{CH4} [c]	S_{N2} [c]	D_{CO2}/D_{CH4}	D_{CO2}/D_{N2}	S_{CO2}/S_{CH4}	S_{CO2}/S_{N2}
SPEEK	4.80	1.33	1.90	3.10	0.41	0.21	3.61	2.53	7.56	14.76
SPEEK/MIL(−101 Cr)-10	5.42	1.73	2.45	3.28	0.37	0.20	3.13	2.05	8.90	16.50
SPEEK/MIL-101(Cr)-20	5.94	2.00	2.95	3.59	0.35	0.19	2.97	2.01	10.29	18.95
SPEEK/MIL-101(Cr)-30	6.43	2.50	3.30	4.01	0.33	0.20	2.57	1.95	12.12	20.00
SPEEK/MIL-101(Cr)-40	6.79	2.84	4.17	4.31	0.32	0.18	2.39	1.65	13.44	20.39
SPEEK/PEI@MIL-101(Cr)-10	5.25	1.48	2.40	3.62	0.44	0.20	3.54	2.19	8.18	18.00
SPEEK/PEI@MIL-101(Cr)-20	5.51	1.46	2.36	4.10	0.48	0.22	3.53	2.33	8.54	18.64
SPEEK/PEI@MIL-101(Cr)-30	5.86	1.68	2.52	4.91	0.50	0.25	3.49	2.33	9.48	19.60
SPEEK/PEI@MIL-101(Cr)-40	6.76	1.82	2.81	5.50	0.50	0.27	3.71	2.41	11.00	20.37

[a]Membranes were tested at 1.5 bar, 25 °C. [b]Diffusivity coefficient [cm^2/s] × 10^8. [c]Solubility coefficient [$cm^3(STP)/cm^3cmHg$] × 10^2.

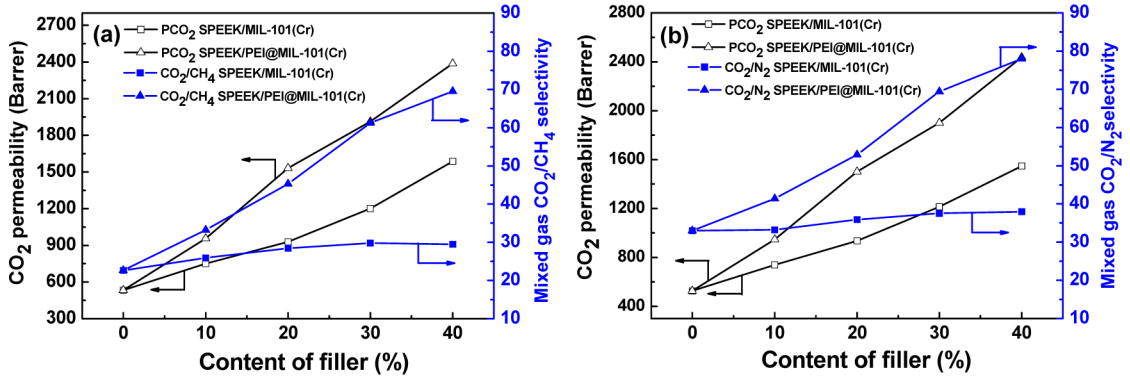

Figure 8. (a) Mixed gas CO_2 permeability and CO_2/CH_4 selectivity; (b) mixed gas CO_2 permeability and CO_2/N_2 selectivity for pristine MIL-101(Cr) and PEI@MIL-101(Cr) based MMMs (1 bar, 25 °C).

attributed to the higher solubility of CO_2 in the MOF particles and faster diffusion through the MOF particles. The electrostatic interaction between CO_2 (strong quadrupole moment) and the open metal sites of chromium cations increased the sorption capacity of CO_2, leading to higher gas sorption. It was previously reported that CO_2 molecules can form coordinated species on Lewis sites in MIL-101.[29] These coordinated sites increased the uptake of CO_2 in the MOFs, and thus increasing the solubility of CO_2 in the membranes. Compared with the membranes doped with pristine MIL-101(Cr), the CO_2 permeability of the PEI@MIL-101(Cr)-doped membranes increased by 53.4% at 40 wt % filler loading. The more pronounced increase in CO_2 permeability of the SPEEK/PEI@MIL-101(Cr) series membranes was due to the following two possible reasons. The higher total water content in the SPEEK/PEI@MIL-101(Cr) membrane than that in the SPEEK/MIL-101 membrane at the same filler content led to an increased CO_2 permeability. Moreover, the enhanced CO_2 permeability might be attributed to the higher solubility of CO_2. As the content of amine groups increased, the transport of CO_2 was more favored.

Both the MMMs loaded with MIL-101(Cr) and PEI@MIL-101(Cr) showed a consistent increase in ideal CO_2/gas selectivity with the increasing filler loading up to 40 wt %. The improved interfacial interactions due to the similar physicochemical properties and acid−base pair interactions between MOFs and SPEEK matrix were vital for high-performance gas separation. Compared with unfilled SPEEK membrane, the enhanced solubility of CO_2 in the SPEEK/MIL-101(Cr) MMMs due to the presence of open chromium cation sites resulted in increased selectivity. Besides, the water molecules in the hydrated MIL-101(Cr) as additional CO_2 adsorption sites led to enhanced selectivity.[47] Compared to SPEEK/MIL-101(Cr)-40 membrane, the SPEEK/PEI@MIL-101(Cr)-40 membrane showed an increment of CO_2/CH_4 and CO_2/N_2 selectivity by 128.1% and 102.4%, respectively. The selectivity of CO_2/gas for the SPEEK/PEI@MIL-101(Cr) MMMs increased more remarkably than for SPEEK/MIL-101(Cr) MMMs at the same loadings because of the following reasons. First, compared to the SPEEK/MIL-101(Cr) MMMs, the increased chain rigidification for the SPEEK/PEI@MIL-101(Cr) MMMs enhanced the CO_2/gas selectivity. Second, compared to the SPEEK/MIL-101(Cr) MMMs, the decreased FFV and the modestly decreased pore size for PEI@MIL-101(Cr) in the SPEEK/PEI@MIL-101(Cr) MMMs suggested fewer diffusion pathways for all gases, especially for larger diameter molecule, and thus led to an increased diffusion selectivity. Third, the SPEEK/PEI@MIL-101(Cr) MMMs possessed higher bound water content than SPEEK/MIL-101(Cr) MMMs leading to higher CO_2/gas selectivity. In addition, it was reported that amine group-modified MOFs showed a significant enhancement for CO_2 adsorption enthalpy and CO_2 adsorption capacity in comparison with unmodified MOFs,[48] and thus the introduction of polyethylenimine into MIL-101(Cr) was inferred to be effective for CO_2-selective adsorption as well as in the enhancement of CO_2 adsorption enthalpy.

To get a further insight into the roles of the fillers and their modification treatment, we measured and calculated diffusion and solubility of the flat sheet homogeneous membranes. As expected, the diffusion coefficient for CO_2 gas increased with increasing filler loadings for both types of MMMs (Table 1). The CO_2 diffusion coefficient increased from 4.8×10^{-8} cm^2/s for unfilled SPEEK membrane to 6.79×10^{-8} cm^2/s and 6.76×10^{-8} cm^2/s for SPEEK/MIL-101(Cr) and SPEEK/PEI@MIL-101(Cr) at the loading of 40 wt %, respectively. The MMMs

DOI: 10.1021/am504742q
ACS Appl. Mater. Interfaces 2015, 7, 1065−1077

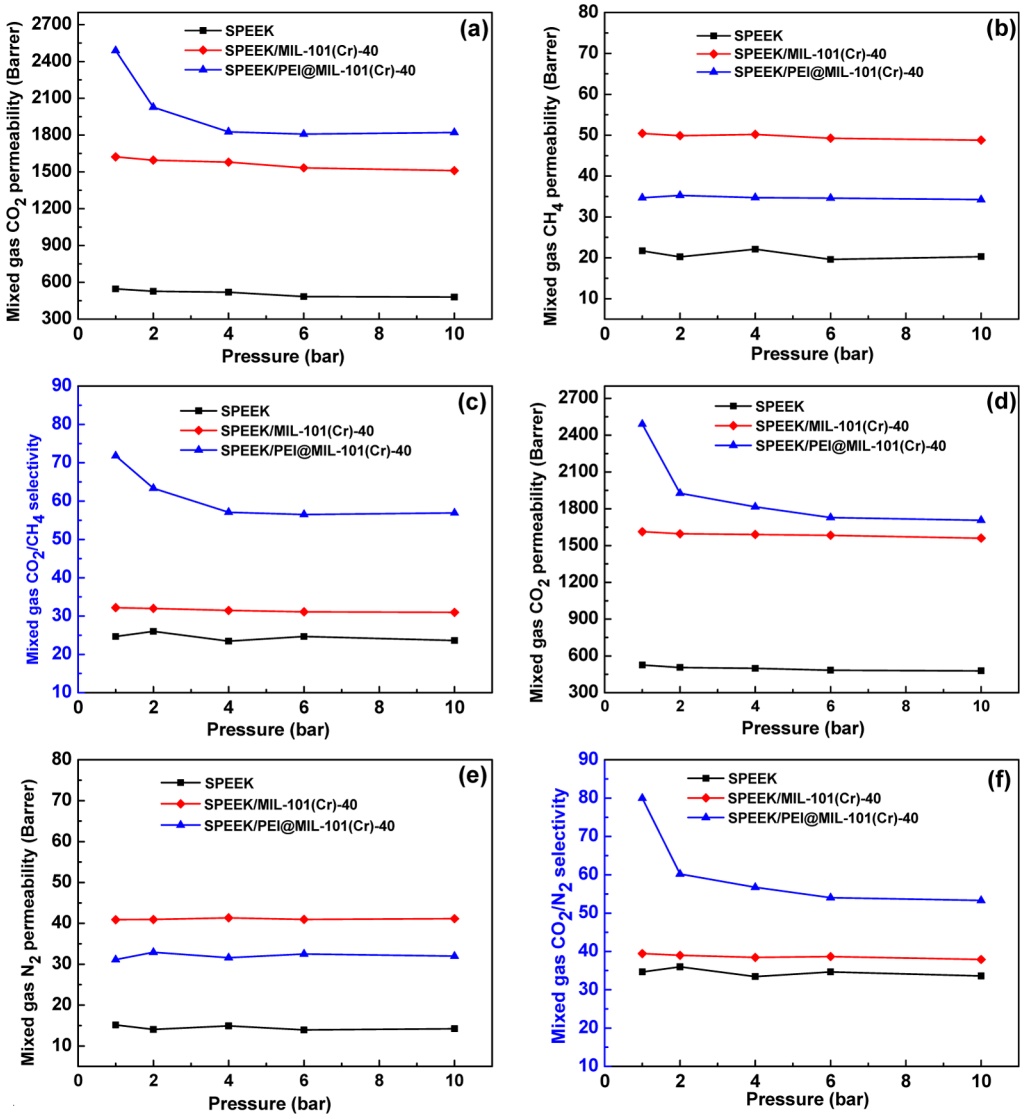

Figure 9. Effect of pressure on (a) mixed gas CO_2 permeability, (b) mixed gas CH_4 permeability, (c) mixed gas CO_2/CH_4 selectivity, (d) mixed gas CO_2 permeability, (e) mixed gas N_2 permeability, (f) mixed gas CO_2/N_2 selectivity of membranes. Permeation tests were performed at 25 °C with humidified feed gas and sweep gas.

loaded with PEI-decorated MOF showed a slightly decrease in diffusivity in comparison to the unmodified MOFs-doped MMMs. This difference in diffusivity was mainly due to the comprehensive effect of decreased chain mobility, decreased FFV and slightly decreased pore size of fillers. Similar to the diffusivity, both the two types of MMMs showed an increased solubility with increasing filler loading. However, in contrast to diffusivity, the SPEEK/PEI@MIL-101(Cr) membranes showed higher solubility than the SPEEK/MIL-101(Cr) membranes. Compared to the unfilled SPEEK membrane, the MMMs loaded with MIL-101(Cr) and PEI@MIL-101(Cr) showed an increased CO_2 solubility coefficient by 39% and 77%, respectively. The SPEEK/PEI@MIL-101(Cr) membranes provided CO_2-facilitated transport sites of amine groups from PEI decorated onto MIL-101(Cr) for the penetrant CO_2 molecules. This increased solubility also explained the difference in the ideal selectivity between the two types of MMMs.

3.4. Mixed Gas Separation Performance. To evaluate the practical separation performance of membranes, we conducted mixed gas permeation tests using CO_2/CH_4 and CO_2/N_2 mixtures as feed gas. CO_2 permeability, CO_2/CH_4, and CO_2/N_2 selectivity results for the unfilled SPEEK membrane, SPEEK/MIL-101(Cr)-40 membrane, and SPEEK/PEI@MIL-101(Cr)-40 membrane are plotted in Figure 8. The mixed gas CO_2/CH_4 selectivity and CO_2/N_2 selectivity of unfilled SPEEK membrane, SPEEK/MIL-101(Cr)-40 membrane, and SPEEK/PEI@MIL-101(Cr)-40 membrane were slightly lower than their corresponding ideal selectivity. This decrease in selectivity was due to the effect of penetrant competition mainly including the competitive sorption and competitive diffusion. However, the mixed gas selectivities of SPEEK/PEI@MIL-101(Cr)-40 membrane for both CO_2/CH_4 and CO_2/N_2 mixtures were almost identical to the ideal selectivities. Many studies have demonstrated a strong affinity between amine groups and CO_2 molecules. Because the incorporation of PEI-decorated MIL-101(Cr) introduced an abundance of amine groups into the membrane, the amount of specific sorption sites for CO_2 multiplied, thus diminishing the penetrant competition effect caused by CH_4 or N_2.

DOI: 10.1021/am504742q
ACS Appl. Mater. Interfaces 2015, 7, 1065−1077

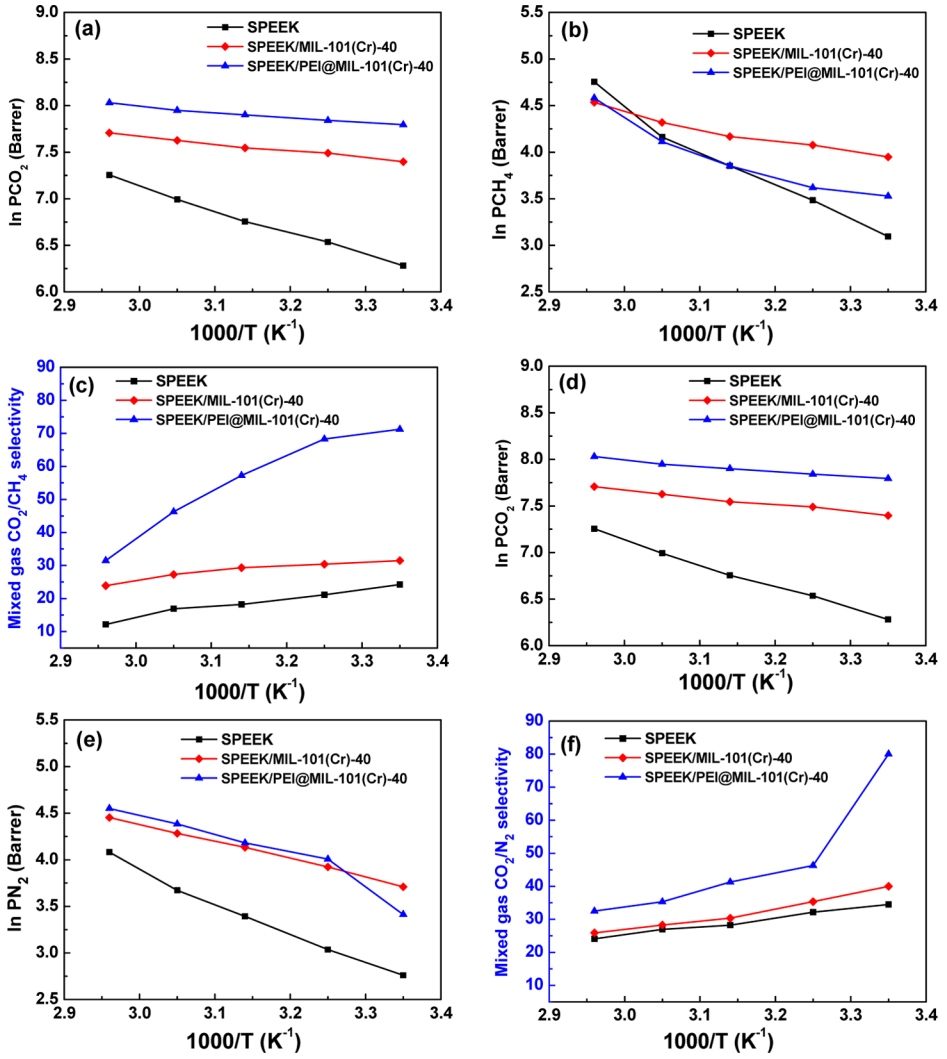

Figure 10. Effect of operating temperature on (a) $LnPCO_2$ (Barrer); (b) $LnPCH_4$ (Barrer); (c) mixed gas CO_2/CH_4 selectivity; (d) $LnPCO_2$ (Barrer); (e) $LnPN_2$ (Barrer); (f) mixed gas CO_2/N_2 selectivity of membranes in mixed feed gases. Permeation tests were performed at 1 bar feed pressure with humidified feed gas and sweep gas.

3.5. Effect of Operating Pressure. The effect of operating pressure on gas separation performance is shown in Figure 9. All the CO_2 permeability, CO_2/CH_4 selectivity, and CO_2/N_2 selectivity decreased with the increase of feed gas pressure, which indicated the presence of facilitated transport mechanism. However, the decline tendency was not obvious as the other amino-containing facilitated membranes when the pressure was higher than 6 bar. That was, in the membranes doped with PEI@MIL-101(Cr), the pores of MOF could serve as CO_2 transport channels and then CO_2 transport was remarkably enhanced in the membrane at high pressure.[49,50] Unlike the CO_2 permeation behavior with pressure, the permeability of CH_4 and N_2 were only slightly changed with increasing feed pressure because the transport of these two gases through the membrane followed the solution-diffusion mechanism, which was independent of the feed gas pressure. If a gas permeates through the membrane following the ideal solution-diffusion mechanism, its permeability is independent of concentration driving force across the membrane.[46]

3.6. Effect of Operating Temperature. Operating temperature is crucial determining the application of membrane. As shown in Figure 10, the gas permeability gradually increased with temperature, whereas the CO_2/gas selectivity decreased with temperature. The CO_2-amine reaction rate and gas diffusivity were accelerated as temperature increased, while gas solubility decreased as temperature increased. The gas separation performance was the comprehensive effect of increased gas diffusivity, decreased gas solubility and promoted reaction between CO_2 and amine groups as temperature increased. The gas permeability increased due to the increased gas diffusivity and CO_2-amine reaction rate. The decreased CO_2/gas selectivity was mainly due to the more rapid diffusion of CH_4 and N_2 molecules than that of CO_2, which led to decreased CO_2/gas diffusivity selectivity with temperature increasing. Nevertheless, the mixed gas CO_2/N_2 selectivity remained as high as 31.5 with a high CO_2 permeability up to 3076 Barrer at 65 °C, which was remarkably higher than the selectivity of unfilled SPEEK (24.2) under the same conditions, displaying encouraging CO_2 separation performance.

The effect of temperature could be further described by using the Arrhenius equation which related the gas permeability to the operating temperature via the activation energy of permeability (E_p) as expressed by the following equation

DOI: 10.1021/am504742q
ACS Appl. Mater. Interfaces 2015, 7, 1065−1077

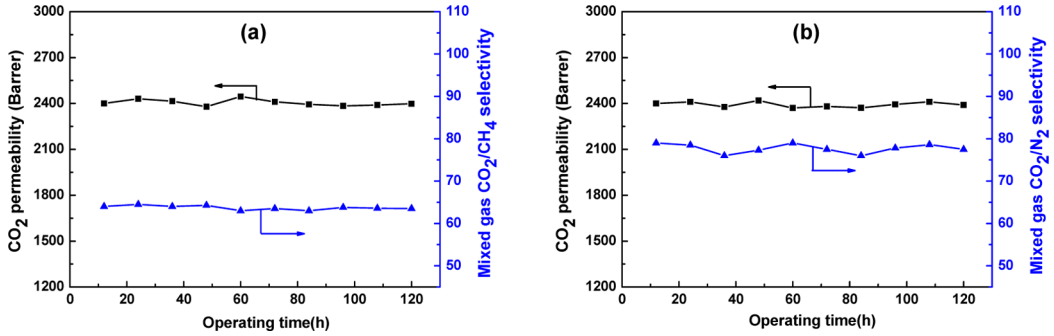

Figure 11. Long-term gas separation performance test of the SPEEK/PEI@MIL-101(Cr)-40 mixed matrix membrane up to 120 h for (a) CO_2/CH_4 and (b) CO_2/N_2 mixtures at 1 bar feed pressure and 25 °C with humidified feed gas and sweep gas.

$$P = P_0 \exp\left(-\frac{E_p}{RT}\right) \quad (5)$$

where P was the permeability of the gas, P_0 the pre-exponential factor, R the gas constant. and T the absolute temperature. The activation energies of CO_2 permeability (E_P) obtained from the slope of ln P vs 1000/T were 21.59, 14.46, and 15.85 kJ/mol for SPEEK, SPEEK/MIL-101(Cr)-40 and SPEEK/PEI@MIL-101(Cr)-40 membranes, respectively. The activation energies of permeability (E_P) significantly decreased for the MMMs at the loading of 40 wt % in comparison with unfilled SPEEK.

3.7. Long-Term Operation Stability. The long-term operation stability is vital to the industrial application of membrane. The long-term gas separation performance of the membrane doped with PEI@MIL-101(Cr) at 40 wt % loading up to 120 h for CO_2/CH_4 and CO_2/N_2 mixtures is shown in Figure 11. During the entire test period, the CO_2 permeability and the selectivities of CO_2/CH_4 and CO_2/N_2 remained stable, indicating a favorable operation stability.

3.8. Comparison with Other MOF-Based Mixed Matrix Membranes in the Literature. Table S3 in the Supporting Information exhibits the CO_2/gas separation performances of MOF-based MMMs reported in literatures and the results in this study. Compared with other MOF-based MMMs in literatures, our results of gas separation performance of MMMs were encouraging. For instance, the gas separation performance of SPEEK/PEI@MIL-101(Cr)-40 membrane in wet state surpassed the 2008 upper bound, displaying that functional groups-decorated MOFs had improved gas separation performance and their adhension with the polymer.

4. CONCLUSIONS

Mixed matrix membranes composed of SPEEK and PEI@MIL-101(Cr) were prepared and their gas separation performances were investigated. MIL-101(Cr) was functionalized with PEI by a facile vacuum-assisted method and the dispersion of PEI in MIL-101(Cr) was uniform. As the content of PEI@MIL-101(Cr) in the membrane increased, the CO_2 permeability, CO_2/CH_4 selectivity, and CO_2/N_2 selectivity were all increased. In particular, the membrane loaded with PEI@MIL-101(Cr) (40 wt %) exhibited the highest selectivities up to 71.8 and 80.0 for CO_2/CH_4 and CO_2/N_2 mixtures, respectively, with a CO_2 permeability of 2490 Barrer at 1.0 bar and 25 °C. This result surpassed the Robeson's upper bound revised in 2008. The incorporation of the PEI@MIL-101(Cr) fillers introduced CO_2-facilitated transport sites to facilitate the selective permeation of CO_2 molecules across the membranes, and the resultant MMMs showed the most significant increments in both CO_2/CH_4 and CO_2/N_2 selectivities compared to those loaded with undecorated MIL-101(Cr) fillers at the same content. The increased selectivity was mainly attributed to the good filler−polymer interface compatibility because of the electrostatic interaction and hydrogen bond between sulfonic acid group and PEI, the increased amount of facilitated transport interaction sites for CO_2 and the decreased fractional free volume (FFV). Moreover, the mechanical and thermal stabilities of MMMs were also enhanced compared to the unfilled SPEEK membrane.

■ ASSOCIATED CONTENT

Ⓢ Supporting Information

Chemical structure of PEI and SPEEK; the open windows and the mesoporous cages of MIL-101(Cr) in the 3D framework; gas permeation apparatus scheme; additional experimental data including spectrum of XRD, SEM, EDX, FT-IR, XPS; the BET result of MIL-101(Cr) and PEI@MIL-101(Cr); TGA result of MIL-101(Cr) and PEI@MIL-101(Cr); leakage ratio of PEI from PEI@MIL-101(Cr); DSC measurement of membranes; mechanical property of membranes; TGA result of membrane; the water uptake and area swelling properties of membranes; dynamic CO_2 separation properties of membranes and FTIR spectra of CO_2 adsorption and desorption within membranes in humidified state. This material is available free of charge via the Internet at http://pubs.acs.org.

■ AUTHOR INFORMATION

Corresponding Author

*E-mail: wuhong@tju.edu.cn. Fax: +86 22 2350 0086. Tel: +86 22 2350 0086.

Author Contributions

The manuscript was written through contributions of all authors. All authors have given approval to the final version of the manuscript.

Notes

The authors declare no competing financial interest.

■ ACKNOWLEDGMENTS

The authors gratefully acknowledge the financial support from the National High Technology Research and Development Program of China (2012AA03A611), Program for New Century Excellent Talents in University (NCET-10-0623), the National Science Fund for Distinguished Young Scholars (21125627), and the Program of Introducing Talents of Discipline to Universities (B06006).

DOI: 10.1021/am504742q
ACS Appl. Mater. Interfaces 2015, 7, 1065−1077

NOMENCLATURE

Symbols

T_g	glass transition temperature (°C)
m_{PEI}	initial weight of PEI@MIL-101(Cr)
ω_n	content of nitrogen element of supernatant liquid separated after the nth circle (wt %, g mL^{-1})
V	volume of water (10 mL)
M_{PEI}, M_N	relative molecular mass of PEI and relative atomic mass of nitrogen (g mol^{-1})
m_n	the leakage of PEI in the nth circle
Σ	summation notation, employed to calculate the total leakage of PEI after the nth circle
ω_{PEI}	PEI content of PEI@MIL-101(Cr) determined by ICP (wt %, g g^{-1})
L_n	Leakage ratio of PEI after the nth circle (%)
r_3	free volume radius (nm)
τ_3	lifetime of o-Ps (ns)
I_3	intensity of o-Ps component (%)
FFV	apparent fractional free volume (%)
Δr	electron layer thickness (nm)
W_d	weight of dry membranes (mg)
W_w	weight of a fully hydrated membrane at constant temperature (mg)
m_1	the weight of membrane after gas permeation test (mg)
m_2	the weight of membrane after 100 °C in a vacuum oven to remove free water (mg)
m_0	the weight of membrane after 150 °C in a vacuum oven to remove bound water (mg)
W_t	content of total water (%)
W_f	content of free water (%)
W_b	content of bound water (%)
W_{dry}	weight of dry membrane (mg)
W_{wet}	weight of fully hydrated membrane (mg)
A_{dry}	area of dry membrane (cm^2)
A_{wet}	area of fully hydrated membrane (cm^2)
P_i	permeability of each gas (Barrer)
Q_i	volumetric flow rate of gas 'i' (cm^3/s (SPT))
l	thickness of the membranes (μm)
Δp_i	transmembrane pressure differencegas constant (cmHg)
$\alpha_{i/j}$	ideal selectivity and mixed gas separation factor of gas "i and j"
D	diffusion coefficient ([cm^2/s] × 10^8)
S	solubility coefficient ([cm^3(STP)/cm^3cmHg] × 10^2)
E_p	the activation energy of permeability (kJ/mol)

Abbreviations

PEI	polyethylenimine
SPEEK	sulfonated poly(ether ether ketone)
MOFs	metal−organic frameworks
COFs	covalent organic frameworks
MIL	materials of Institut Lavoisier
HADDF	high-angle angular dark field

REFERENCES

(1) Gin, D. L.; Noble, R. D. Designing the Next Generation of Chemical Separation Membranes. *Science* **2011**, *332*, 674−676.

(2) Robeson, L. M. The Upper Bound Revisited. *J. Membr. Sci.* **2008**, *320*, 390−400.

(3) Maier, G. Gas Separation with Polymer Membranes. *Angew. Chem., Int. Ed.* **1998**, *37*, 2960−2974.

(4) Zhang, Y.; Sunarso, J.; Liu, S. M.; Wang, R. Current Status and Development of Membranes for CO_2/CH_4 Separation: A Review. *Int. J. Greenhouse Gas Control* **2013**, *12*, 84−107.

(5) Du, N.; Park, H. B.; Dal-Cin, M. M.; Guiver, M. D. Advances in High Permeability Polymeric Membrane Materials for CO_2 Separations. *Energy Environ. Sci.* **2012**, *5*, 7306−7322.

(6) Gascon, J.; Kapteijn, F.; Zornoza, B.; Sebastian, V.; Casado, C.; Coronas, J. Practical Approach to Zeolitic Membranes and Coatings: State of the Art, Opportunities, Barriers, and Future Perspectives. *Chem. Mater.* **2012**, *24*, 2829−2844.

(7) Li, Y. F.; He, G. W.; Wang, S. F.; Yu, S. N.; Pan, F. S.; Wu, H.; Jiang, Z. Y. Recent Advances in the Fabrication of Advanced Composite Membranes. *J. Mater. Chem. A* **2013**, *1*, 10058−10077.

(8) Merkel, T. C.; Freeman, B. D.; Spontak, R. J.; He, Z.; Pinna, I.; Meakin, P.; Hill, A. J. Ultrapermeable, Reverse-Selective Nanocomposite Membranes. *Science* **2002**, *296*, 519−552.

(9) Joly, C.; Smaihi, M.; Porcar, L.; Noble, R. D. Polyimide−Silica Composite Materials: How Does Silica Influence Their Microstructure and Gas Permeation Properties? *Chem. Mater.* **1999**, *11*, 2331−2338.

(10) Ahmad, J.; Hägg, M. B. Preparation and Characterization of Polyvinylacetate/ Zeolite 4A Mixed Matrix Membrane for Gas Separation. *J. Membr. Sci.* **2013**, *427*, 73−84.

(11) Lee, Y.; Liu, D.; Seoung, D.; Liu, Z.; Kao, C. C.; Vogt, T. Pressure-and Heat-Induced Insertion of CO_2 into an Auxetic Small-Pore Zeolite. *J. Am. Chem. Soc.* **2011**, *133*, 1674−1677.

(12) Vu, D. Q.; Koros, W. J.; Miller, S. J. Mixed Matrix Membranes Using Carbon Molecular Sieves: I. Preparation and Experimental Results. *J. Membr. Sci.* **2003**, *211*, 311−334.

(13) Sayari, A.; Belmabkhout, Y. Stabilization of Amine-Containing CO_2 Adsorbents: Dramatic Effect of Water Vapor. *J. Am. Chem. Soc.* **2010**, *132*, 6312−6314.

(14) Dai, Y.; Johnson, J. R.; Karvan, O.; Sholl, D. S.; Koros, W. J. Ultems/ZIF-8 Mixed Matrix Hollow Fiber Membranes for CO_2/N_2 Separations. *J. Membr. Sci.* **2012**, *401−402*, 76−82.

(15) Díaz, K.; López-González, M.; Del Castillo, L. F.; Riande, E. Effect of Zeolitic Imidazolate Frameworks on the Gas Transport Performance of ZIF-8-poly(1,4- phenyleneether-ether-sulfone) Hybrid Membranes. *J. Membr. Sci.* **2011**, *383*, 206−213.

(16) Yang, Q. Y.; Zhong, C. L. Molecular Simulation of Carbon Dioxide/Methane/ Hydrogen Mixture Adsorption in Metal−Organic Frameworks. *J. Phys. Chem. B* **2006**, *110*, 17776−17783.

(17) Perez, E. V.; Balkus, K. J.; Ferraris, J. P.; Musselman, I. H. Mixed-Matrix Membranes Containing MOF-5 for Gas Separations. *J. Membr. Sci.* **2009**, *328*, 165−173.

(18) Adams, R.; Carson, C.; Ward, J.; Tannenbaum, R.; Koros, W. Metal Organic Framework Mixed Matrix Membranes for Gas Separations. *Microporous Mesoporous Mater.* **2010**, *131*, 13−20.

(19) Bae, T. H.; Lee, J. S.; William, W. Q.; Koros, W. J.; Jones, C. W.; Nair, S. A High-Performance Gas-Separation Membrane Containing Submicrometer-Sized Metal-Organic Framework Crystals. *Angew. Chem., Int. Ed.* **2010**, *49*, 9863−9866.

(20) Basu, S.; Cano-Odena, A.; Vankelecom, I. F. J. Asymmetric Matrimid®/$[Cu_3(BTC)_2]$ Mixed-Matrix Membranes for Gas Separations. *J. Membr. Sci.* **2010**, *362*, 478−487.

(21) Bae, T. H.; Long, J. R. CO_2/N_2 Separations with Mixed-Matrix Membranes Containing Mg_2(dobdc) Nanocrystals. *Energy Environ. Sci.* **2013**, *6*, 3565−3569.

(22) Song, Q. L.; Nataraj, S. K.; Roussenova, M. V.; Tan, J. C.; Hughes, D. J.; Li, W.; Bourgoin, P.; M. Alam, A. A.; Cheetham, K.; Al-Muhtaseb, S. A.; Sivaniah, E. Zeolitic Imidazolate Framework (ZIF-8) Based Polymer Nanocomposite Membranes for Gas Separation. *Energy Environ. Sci.* **2012**, *5*, 8359−8369.

(23) Hu, J.; Cai, H. P.; Ren, H. Q.; Wei, Y. M.; Xu, Z. L.; Liu, H. L.; Hu, Y. Mixed-Matrix Membrane Hollow Fibers of $Cu_3(BTC)_2$ MOF and Polyimide for Gas Separation and Adsorption. *Ind. Eng. Chem. Res.* **2010**, *49*, 12605−12612.

(24) Wang, Z. Q.; Cohen, S. M. Postsynthetic Modification of Metal−Organic Frameworks. *Chem. Soc. Rev.* **2009**, *38*, 1315−1329.

DOI: 10.1021/am504742q
ACS Appl. Mater. Interfaces 2015, 7, 1065−1077

(25) Basu, S.; Cano-Odena, A.; Vankelecom, I. F. J. MOF-Containing Mixed-Matrix Membranes for CO_2/CH_4 and CO_2/N_2 Binary Gas Mixture Separations. *Sep. Sci. Technol.* **2011**, *81*, 31−40.
(26) Zhang, Y. F.; Musselman, I. H.; Ferraris, J. P.; Balkus, K. J. B., Jr Gas Permeability Properties of Matrimid® Membranes Containing the Metal−Organic Framework Cu-BPY-HFS. *J. Membr. Sci.* **2008**, *313*, 170−181.
(27) Zornoza, B.; Martinez-Joaristi, A.; Serra-Crespo, P.; Téllez, C.; Coronas, J.; Gascon, J.; Kapteijn, F. Functionalized Flexible MOFs as Fillers in Mixed Matrix Membranes for Highly Selective Separation of CO_2 from CH_4 at Elevated Pressures. *Chem. Commun.* **2011**, *47*, 9522−9524.
(28) Férey, G.; Mellot-Draznieks, C.; Serre, C.; Millange, F.; Dutour, J.; Surblé, S.; Margiolaki, I. A Chromium Terephthalate-Based Solid with Unusually Large Pore Volumes and Surface Area. *Science* **2005**, *309*, 2040−2042.
(29) Llewellyn, P. L.; Bourrelly, S.; Serre, C.; Vimont, A.; Daturi, M.; Hamon, L.; De Weireld, G.; Chang, J. S.; Hong, D. Y.; Hwang, Y. K.; Jhung, S. H.; Férey, G. High Uptakes of CO_2 and CH_4 in Mesoporous Metal-Organic Frameworks MIL-100 and MIL-101. *Langmuir* **2008**, *24*, 7245−7250.
(30) Caro, J. Are MOF Membranes Better in Gas Separation than Those Made of Zeolites? *Curr. Opin. Chem. Eng.* **2011**, *1*, 77−83.
(31) Xuan, W. M.; Zhu, C. F.; Liu, Y.; Cui, Y. Mesoporous Metal−Organic Framework Materials. *Chem. Soc. Rev.* **2012**, *41*, 1677−1695.
(32) Jeazet, H. B. T.; Staudt, C.; Janiak, C. A Method for Increasing Permeability in O_2/N_2 Separation with Mixed-Matrix Membranes Made of Water-Stable MIL-101 and Polysulfone. *Chem. Commun.* **2012**, *48*, 2140−2142.
(33) Chen, X. Y.; Vinh-Thang, H.; Rodrigue, D.; Kaliaguine, S. Amine-Functionalized MIL-53 Metal−Organic Framework in Polyimide Mixed Matrix Membranes for CO_2/CH_4 Separation. *Ind. Eng. Chem. Res.* **2012**, *51*, 6895−6906.
(34) Thompson, J. A.; Brunelli, N. A.; Lively, R. P.; Johnson, J. R.; Jones, C. W.; Nair, S. Tunable CO_2 Adsorbents by Mixed-Linker Synthesis and Postsynthetic Modification of Zeolitic Imidazolate Frameworks. *J. Phys. Chem. C* **2013**, *117*, 8198−8207.
(35) Couck, S.; Denayer, J. F. M.; Baron, G. V.; Rémy, T.; Gascon, J.; Kapteijn, F. An Amine-Functionalized MIL-53 Metal-Organic Framework with Large Separation Power for CO_2 and CH_4. *J. Am. Chem. Soc.* **2009**, *131*, 6326−6327.
(36) Khutia, A.; Janiak, C. Programming MIL-101Cr for Selective and Enhanced CO_2 Adsorption at Low Pressure by Postsynthetic Amine Functionalization. *Dalton Trans.* **2014**, *43*, 1338−1347.
(37) Hu, Y. L.; Verdegaal, W. M.; Yu, S. H.; Jiang, H. L. Alkylamine-Tethered Stable Metal−Organic Framework for CO_2 Capture from Flue Gas, Alkylamine-Tethered Stable Metal−Organic Framework for CO_2 Capture from Flue Gas. *ChemSusChem* **2014**, *7*, 734−737.
(38) Yan, Q. J.; Lin, Y. C.; Kong, C. L.; Chen, L. Remarkable CO_2/CH_4 Selectivity and CO_2 Adsorption Capacity Exhibited by Polyamine-Decorated Metal−Organic Framework Adsorbents. *Chem. Commun.* **2013**, *49*, 6873−6875.
(39) Khan, A. L.; Klaysom, C.; Gahlaut, A.; Li, X. F.; Vankelecom, I. F. J. SPEEK and Functionalized Mesoporous MCM-41 Mixed Matrix Membranes for CO_2 Separations. *J. Mater. Chem.* **2012**, *22*, 20057−20064.
(40) Sijbesm, H.; Nymeijer, K.; Marwijk, R.; Heijboer, R.; Potreck, J.; Wessling, M. Flue Gas Dehydration Using Polymer Membranes. *J. Membr. Sci.* **2008**, *313*, 263−276.
(41) Chai, Z.; Wang, C.; Zhang, H.; Doherty, C. M.; Ladewig, B. P.; Hill, A. J.; Wang, H. Nafion-Carbon Nanocomposite Membranes Prepared Using Hydrothermal Carbonization for Proton-Exchange-Membrane Fuel Cells. *Adv. Funct. Mater.* **2010**, *20*, 4394−4399.
(42) Bae, B.; Ha, H. Y.; Kim, D. Preparation and Characterization of Nafion/Poly (1-vinylimidazole) Composite Membrane for Direct Methanol Fuel Cell Application. *J. Electrochem. Soc.* **2005**, *152*, A1366−A1372.
(43) Totsatitpaisan, P.; Nunes, S. P.; Tashiro, K.; Chirachanchai, S. Investigation of the Role of Benzimidazole-Based Model Compounds on Thermal Stability and Anhydrous Proton Conductivity of Sulfonated Poly(Ether Ether Ketone). *Solid State Ionics* **2009**, *180*, 738−745.
(44) Kerres, J.; Ullrich, A.; Meier, F.; Härin, T. Synthesis and Characterization of Novel Acid-Base Polymer Blends for Application in Membrane Fuel Cells. *Solid State Ionics* **1999**, *125*, 243−249.
(45) Wang, Z.; Li, M.; Cai, Y.; Wang, J. X.; Wang, S. C. Novel CO_2 Selectively Permeating Membranes Containing PETEDA Dendrimer. *J. Membr. Sci.* **2007**, *290*, 250−258.
(46) Wang, M. M.; Wang, Z.; Wang, J. X.; Zhu, Y. Q.; Wang, S. C. An Antioxidative Composite Membrane with the Carboxylate Group as a Fixed Carrier for CO_2 Separation from Flue Gas. *Energy Environ. Sci.* **2011**, *4*, 3955−3959.
(47) Chen, Y. F.; Babarao, R.; Sandler, S. I.; Jiang, J. W. Metal-Organic Framework MIL-101 for Adsorption and Effect of Terminal Water Molecules: From Quantum Mechanics to Molecular Simulation. *Langmuir* **2010**, *26*, 8743−8750.
(48) McDonald, T. M.; D'Alessandro, D. M.; Krishna, R.; Long, J. R. Enhanced Carbon Dioxide Capture upon Incorporation of N,N′-dimethylethylenediamine in the Metal−Organic Framework CuBTTri. *Chem. Sci.* **2011**, *2*, 2022−2028.
(49) Qiao, Z. H.; Wang, Z.; Ma, Z. J.; Zhao, S.; Yuan, S. J.; Wang, J. X.; Wang, S. C. Rational Design of High Performance CO_2 Separation Membrane at High Pressure Using Polymer-Induced Metal Organic Framework Well-Dispersed into the PVAm Membrane. *Angew. Chem., Int. Ed.* **2014**, DOI: 10.1002/anie.201403718.
(50) Bae, Y. S.; Snurr, R. Q. Molecular Simulations of Very High Pressure Hydrogen Storage Using Metal−Organic Frameworks. *Microporous Mesoporous Mater.* **2010**, *135*, 178−186.

DOI: 10.1021/am504742q
ACS Appl. Mater. Interfaces 2015, 7, 1065−1077